Facing channel calibration issues affecting passive radar DPCA and STAP for GMTI

Giovanni Paolo Blasone, Fabiola Colone and Pierfrancesco Lombardo
Dept. of Information Engineering, Electronics and Telecommunications (DIET)
Sapienza University of Rome, Via Eudossiana, 18 - 00184 Rome, Italy
Email: {giovannipaolo.blasone, fabiola.colone, pierfrancesco.lombardo}@uniroma1.it

***Abstract*—This paper addresses the problem of clutter cancellation for ground moving target indication (GMTI) in multi-channel passive radar on mobile platforms. Specifically, the advantages of a space-time adaptive processing (STAP) approach are presented, compared to a displaced phase centre antenna (DPCA) approach, in the case of an angle-dependent imbalance affecting the receiving channels. The schemes are tested against simulated clutter data. Finally, a space-time GLRT detection scheme is proposed, where steering vector is not specified in the spatial domain, resulting in a non-coherent integration of target echoes across the receiving channels. Such solution offers comparable clutter cancellation capability and is more robust against significant calibration errors compared to a conventional GLRT detector, which suffers from spatial steering vector mismatches.**

Keywords—passive radar, DPCA, STAP, channel imbalance.

I. INTRODUCTION

In the last few years, passive radar has gained considerable attention in the scientific community and recent developments have opened new interesting areas of research [1]-[2]. Among them, the application of passive radar technology to moving platforms is one of the most innovative and challenging.

The use of passive radar on mobile platform could extend the functionalities of this type of sensors to applications like synthetic aperture radar (SAR) imaging or ground moving target indication (GMTI). Moreover, it could bring the typical advantages of passive radar to airborne class systems.

The strategic advantages of a mobile passive radar are paid in terms of motion induced Doppler distortions of received signal. In particular, the Doppler-spread backscattering from stationary scene can hinder the detection of moving targets with small radial velocity component, appearing as buried into clutter. This effect tends to be even more stressed at the VHF/UHF bands of the most widely used illuminators of opportunity, due to the typical broad antenna beams available. The detection of slow-moving targets requires then a proper suppression of clutter echoes, which can be achieved by exploiting systems with multiple receiving channels, enabling space-time processing.

First attempts of providing passive radar with GMTI capability exploited the displaced phase centre antenna (DPCA) approach [4]-[10]. DPCA performs a non-adaptive subtraction of radar echoes collected by two along-track displaced receiving channels at the time that their two-way phase centres occupy the same spatial position [3]. Thus, it requires a simple architecture and limited computational load, which make it attractive for the passive radar application.

A first proof of concept of DPCA in mobile passive radar is given in [4]-[5], for experimental data from an airborne FM-based passive radar and against simulated DVB-T data.

In [7], an effective processing scheme is proposed, based on a reciprocal range compression filter in conjunction with a flexible DPCA approach, which removes the performance limitations deriving from the uncontrolled waveform variability. Its effectiveness is proved for a DVB-T based passive radar against both simulated and experimental data.

However, in [8]-[9], we show that significant performance limitations may come from the presence of amplitude and/or phase imbalance between receiving channels. Such imbalance can be in general function of the angle of arrival, due to several factors: dissimilarities between receiving antennas, mutual coupling effects, interaction with near-field obstacles.

Channel imbalance is a well-known issue in conventional active radar. For specific applications, accurate factory or in-field calibration might be not sufficient or feasible. Strategies for adaptive digital channel calibration based on the received data are proposed in [11]-[12] for the case of SAR-GMTI. In [10], effective solutions are developed to face the critical aspects of the passive radar case. Such solutions prove to be largely required to preserve clutter suppression capability against the imbalance observed in experimental data.

The intrinsic limitations of DPCA and its reliance on an adaptive channel calibration stage for the compensation of localized errors, suggest moving in the direction of an adaptive space-time processing (STAP) approach.

An application of STAP in mobile passive radar is shown with simulated data in [4]; some experimental results are presented in [13], for a DVB-T based passive radar.

In this paper, a STAP approach is considered as an alternative solution to DPCA. At the expense of a higher computational cost, it offers more flexibility and adaptation capability, thanks to a higher number of degrees of freedom. DPCA and STAP are compared in terms of clutter cancellation capability and the advantages of a STAP approach are highlighted, in the case of an angle-dependent imbalance affecting the receiving channels.

Finally, a partially non-coherent GLRT detection scheme is proposed, where steering vector is not specified in the spatial domain, as a simple solution to cope with losses due to target spatial steering vector mismatches. This approach proves to better preserve the moving target echoes when a significant channel imbalance affects the received signals.

The paper is organized as follows. In Section II, the adopted signal model and processing scheme are defined. In Section III, DPCA and STAP approaches are tested and compared against simulated clutter data. In Section IV, coherent and non-coherent GLRT detectors are compared for a post-Doppler STAP approach in the presence of an angle-dependent channel imbalance. Finally, conclusions are drawn in Section V.

II. SIGNAL MODEL AND PROCESSING SCHEME

Let's consider a N channel passive radar receiver mounted on a moving platform and exploiting a stationary transmitter as illuminator of opportunity (see Fig. 1). The platform moves at constant velocity v_p on a straight-line trajectory, assumed without loss of generality along the *x*-axis. Angles φ and ϑ indicate respectively the azimuth and depression angle of the receiver to scatterer line of sight.

By recalling the signal model adopted in [7], the discrete time baseband signal representing the clutter contribution can be expressed as the superposition of echoes from stationary scatterers at different bistatic ranges R_q $(q = 1, \dots, N_R)$ and different angles φ. In particular, for a linear array of elements equally spaced by d, in side-looking configuration (crab angle $\psi = 0$), the clutter contribution received at the *i*-th antenna is:

$$r_C^{(i)}[l] = \sum_{q=1}^{N_R} \int_{\phi} G^{(i)}(\varphi,\vartheta)\, A_q(\varphi) \sum_n s_n\left[l - nL - l_{\tau_q}\right] \cdot \cdot e^{j2\pi \frac{v_p}{\lambda}\cos\varphi\cos\vartheta\, nT}\, e^{-j2\pi\, i\frac{d}{\lambda}\cos\varphi\cos\vartheta}\, d\varphi \quad (1)$$

where

- transmitted signal is partitioned in batches of duration $T$and $s_n[l]$ is the *n*-th batch, including $L = Tf_s$ samples, f_s being the sampling frequency; notice that Doppler induced phase term within each batch has been neglected;
- $\tau_q = l_{\tau_q}/f_s$ is the bistatic propagation delay of echo from clutter patches at range R_q;
- $A_q(\varphi)$ and $G^{(i)}(\varphi,\vartheta)$ are the scatterer complex amplitude and the complex gain of the *i*-th channel, respectively; the latter represents the overall receiver chains, there including the antenna pattern, and encodes possible imbalance between channels;
- $\frac{v_p}{\lambda}\cos\varphi\cos\vartheta$ is the bistatic Doppler frequency of the generic clutter patch at angles (φ,ϑ), λ being the signal carrier wavelength.

The corresponding received signal from a moving target at angles (φ_0,ϑ_0) and bistatic radial velocity v_b, is:

$$r_0^{(i)}[l] = G^{(i)}(\varphi_0,\vartheta_0)\, A_0 \sum_n s_n\left[l - nL - l_{\tau_0}\right] \cdot \cdot e^{j2\pi\, f_D\, nT}\, e^{-j2\pi\, i\frac{d}{\lambda}\cos\varphi_0\cos\vartheta_0} \quad (2)$$

where A_0 is the target complex amplitude and $l_{\tau_0} = f_s R_b/c$ is its bistatic propagation delay. Target bistatic Doppler frequency f_D is given by:

$$f_D = \frac{v_p}{\lambda}\cos\varphi_0\cos\vartheta_0 - \frac{v_b}{\lambda} \quad (3)$$

The simplest space-time approach aimed at clutter cancellation and moving target detection is given by DPCA, where a non-adaptive subtraction is performed between properly delayed observations from two receiving channels.

We consider the processing scheme proposed in [7] for the application of the DPCA approach in a passive radar scenario. The scheme is based on a batches processing architecture, which recreates the conventional fast-time/slow-time framework of a pulsed radar. The range compression stage is performed by means of a reciprocal filter, which has the dual role of controlling the signal ambiguity function and removing the limitation due to the temporal variability of the employed opportunity waveform, so that an ideal cancellation can be in principle obtained based on subsequent observations of a stationary scene.

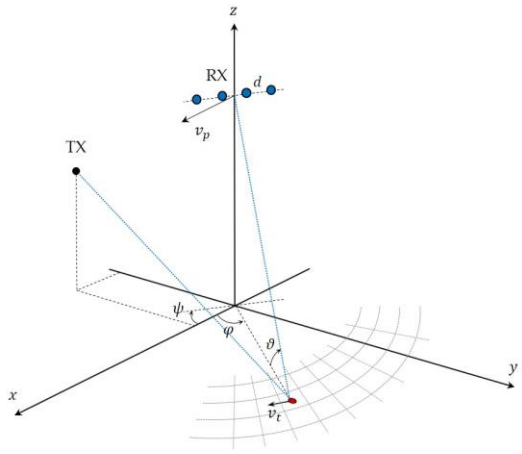

Fig. 1. System geometry for a multichannel mobile passive radar exploiting a stationary transmitter as illuminator of opportunity.

However, as mentioned, significant limitations to the DPCA performance may come from the presence of inter-channel imbalance, which is in general function of the angle of arrival. Adaptive digital channel calibration techniques, like those analysed in [10], are then required to mitigate this problem by compensating for the angle-dependent channel errors. These limitations of the DPCA approach and the need for a localized adaptation capability, lead towards the adoption of a more sophisticated but more flexible adaptive space-time processing (STAP) solution.

STAP adaptively combines spatial and temporal samples of the signal, to suppress clutter in the angle-Doppler domain and maximize the detection probability of potential moving targets [3]. It is based on the inversion of a space-time disturbance covariance matrix $\boldsymbol{Q}$, which is usually not available and has to be estimated based on training data. In order to reduce the computational effort and the amount of training data required for an effective estimation of $\boldsymbol{Q}$, a number of reduced-order STAP approaches have been suggested, where adaptive processing is applied after a non-adaptive projection of data in a proper subspace [14].

Particularly suitable for passive radar case, characterized by relatively long integration times, are the post-Doppler approaches, where adaptation occurs on a subset of Doppler-processed data. Starting from the scheme in [7], the processing scheme for the application of a post-Doppler STAP approach to passive radar framework is sketched in Fig. 2, for the generic case of a N channel receiver.

Specifically, we consider an adjacent-bin post-Doppler (ABPD) approach, which adaptively combines the N spatial samples from L adjacent Doppler bins centred at the bin under test. Calling $\boldsymbol{x}$ the space-Doppler data vector of size $(NL \times 1)$ from the cell under test, possibly including the useful target signal, and $\boldsymbol{s}$ the corresponding space-Doppler steering vector, the well-known optimum filter is given by:

$$z = \boldsymbol{s}^H \boldsymbol{Q}^{-1} \boldsymbol{x} \quad (4)$$

where subscript H denote the Hermitian transpose.

In practical applications, matrix $\boldsymbol{Q}$ is substituted by its ML estimate $\widehat{\boldsymbol{Q}} = \boldsymbol{X}_k \boldsymbol{X}_k^H$, where $\boldsymbol{X}_k = [\boldsymbol{x}_1, \dots, \boldsymbol{x}_K]$ is a set of training data of size $(NL \times K)$ from K adjacent range cells, assumed as statistically independent and target-free. Accordingly, an appropriate threshold is defined to guarantee CFAR property.

Such solution has a higher computational cost compared to DPCA, since requires the estimation and inversion of a covariance matrix of dimension $(NL \times NL)$, potentially for each range-Doppler bin. On the other hand, it can handle a higher number of degrees of freedom, offering more flexibility and adaptation capability.

In the next section, we compare results obtained with DPCA and STAP approaches in a simulated clutter case, for a dual channel passive radar in presence of an angle dependent channel imbalance.

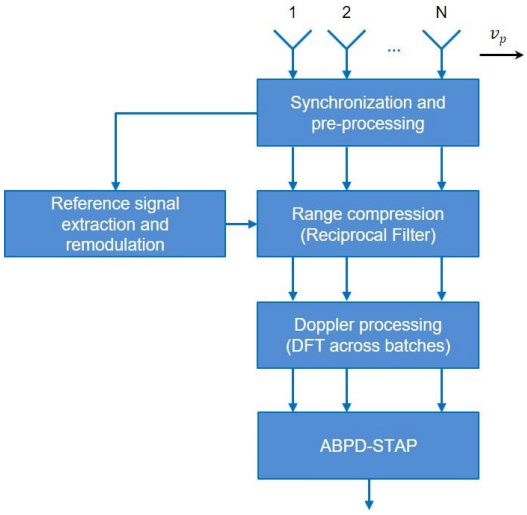

Fig. 2. Sketch of the processing scheme for a post-Doppler STAP approach in passive radar.

III. Comparison of DPCA and STAP approaches

In order to test and compare the considered space-time processing schemes in a controlled environment, we consider a simulated clutter scenario for a mobile passive radar.

We assume a ground moving receiver exploiting a stationary transmitter in a quasi-monostatic geometry. An 8k mode DVB-T signal sequence is generated as reference signal. Clutter returns are generated according to (1), for a scene spanning $N_R = 250$ range cells. For simplicity, amplitudes $A_q(\varphi)$ associated with different clutter patches are assumed independent and identically distributed complex Gaussian, resulting in a homogeneous clutter scenario. Omnidirectional antennas are assumed, within an angular sector $\varphi = [0, \pi]$ (no back-lobe contributions). Carrier frequency is set to 690 MHz, platform velocity $v_p = 13$ m/s and antenna element spacing $d = \lambda/2$. A coherent processing interval (CPI) length of 512 OFDM symbols is considered.

The input signal includes clutter returns, thermal noise (whose level is deliberately set to unity) and the echo from a moving target with bistatic range $R_b = 4$ km, azimuth angle of arrival $\varphi_0 = 90°$ and bistatic radial velocity $v_b = 8$ m/s. The generated signal is scaled so that the overall clutter contribution has an assigned power level of 20 dB above thermal noise level, at the input of each Rx channel. Target signal power level is selected to be -35 dB below noise.

The range-Doppler map obtained from a single channel is reported in Fig. 3. As apparent, clutter returns appear across a Doppler extension of approximately $\pm v_p/\lambda \cong \pm 30\,Hz$, while target signal to clutter plus noise ratio (SCNR) is -22 dB. Notice that range-Doppler maps are scaled to provide unitary processing gain for thermal noise, thus allowing a direct comparison of results. Target SCNR is measured by taking the power level at the target range-Doppler location, when the processing is fed with target echo only, and disturbance power level estimated over a proper area surrounding target location, in the maps containing only clutter and noise.

Assuming the availability of N = 2 receiving channels and applying the considered DPCA scheme from [7], the resulting range-Doppler map at the output is shown in Fig. 4. As evident, the clutter background is completely removed and resulting target SCNR is 24 dB, with an improvement of 46 dB. This result is made possible by the absence of internal clutter motion (ICM), the use of reciprocal filtering and perfectly balanced receiving channels.

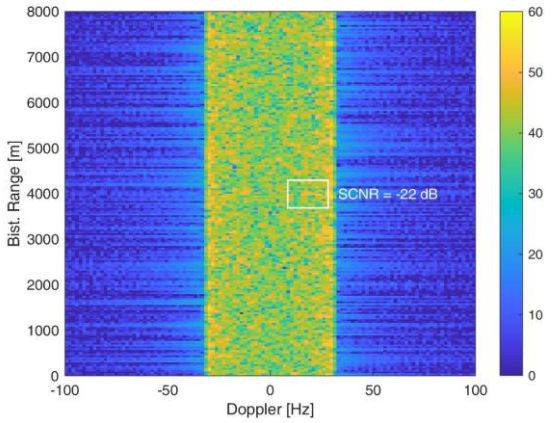

Fig. 3. Single channel range-Doppler map of simulated clutter scenario.

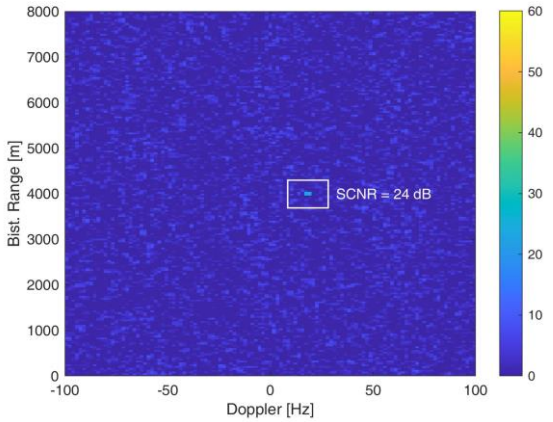

Fig. 4. Range-Doppler map after DPCA in absence of channel imbalance.

In order to analyse the effects of channel imbalance on clutter cancellation performance, we now include in the simulation process the presence of an angle dependent imbalance $\Gamma_{12}(\phi) = G^1(\phi)/G^2(\phi)$ between the two receiving channels. Specifically, we assume a sinusoidal phase imbalance as illustrated in Fig. 5. Notice that, for simplicity, channel imbalance is assumed as a function of the angle ϕ between the array line and the receiver to scatterer line of sight ($\cos\phi = \cos\varphi \cos\vartheta$).

Range-Doppler map resulting at the output of the DPCA stage, when no channel calibration strategy is applied, is shown in Fig. 6(a). As expected, strong clutter residuals are present, limiting the final target SCNR to -1 dB. Notice that the fluctuation of imbalance with the angle is mapped over Doppler frequency, leading to better cancellation capability where the phase imbalance is close to zero.

In order to compensate for the imbalance effect and improve the cancellation performance, a digital channel calibration can be applied, directly operating on the range-Doppler maps, before DPCA subtraction. Specifically, we consider the Doppler dependent calibration (DDC) approach presented in [10], which exploits the duality between angle of arrival and Doppler frequency of stationary scatterers. A set of complex correction coefficients is estimated and separately applied at each Doppler bin within the endo-clutter region, so as to minimize the output clutter power.

The calibration coefficient at the *m*-th Doppler bin is estimated, according to a least square approach, as:

$$\widehat{\Gamma_c}[m] = \frac{\sum_{l=l_1}^{l_2} z^{(1)}[l,m]\, z^{(2)^*}[l,m]}{\sum_{l=l_1}^{l_2} |z^{(2)}[l,m]|^2} \qquad (5)$$

where $z^{(i)}[l,m]$ is the complex value at the generic range-Doppler bin of the *i*-th channel; the average is evaluated over consecutive range cells spanning indexes from l_1 to l_2; channel 1 is arbitrarily taken as reference and channel 2 is adjusted by multiplication with $\widehat{\Gamma_c}[m]$.

Range-Doppler map obtained after DDC calibration and DPCA subtraction is shown in Fig. 6(b). A significant improvement in terms of clutter cancellation performance is achieved, compared to results in Fig. 6(a). Nevertheless, some clutter residuals are still visible in the final map and target SCNR is brought to 11 dB. This is due to the interfering effect between scatterers located at different Doppler frequencies and hence associated to different imbalance values. In fact, residuals are stronger at the edge of clutter Doppler bandwidth, where the Doppler resolution maps into a broader angular resolution. Moreover, this effect would increase with the increase of channel imbalance variation in angle.

Applying the ABPD-STAP scheme in Fig. 2 to the same two-channel case of previous example, the resulting range-Doppler map at the output of the adaptive filter in (4) is shown in Fig. 7. In particular, $L = 3$ adjacent Doppler bins are used, for a total on $NL = 6$ degrees of freedom, and the number of training data is set to $K = 36$. No preliminary channel calibration is applied.

As expected, the adaptation capability of a post-Doppler STAP approach allows to intrinsically compensate for the angle dependent channel imbalance and yields to a significant cancellation of clutter echoes. The final target SCNR is 23 dB, demonstrating the effectiveness of the considered scheme.

Notice that the superiority of a STAP approach compared to a simple DPCA scheme is not a foregone conclusion in a real scenario, where a non-homogeneous clutter might not offer a sufficient number of relevant secondary data

In addition, although the STAP approach is robust against the presence of channel imbalance between receiving channels for what concerns clutter cancellation capability, the same can not be said for the corresponding target steering vector to be used in the adaptive filter. This aspect will be better discussed in the next section, where a partially non-coherent detection scheme is proposed as a potential solution.

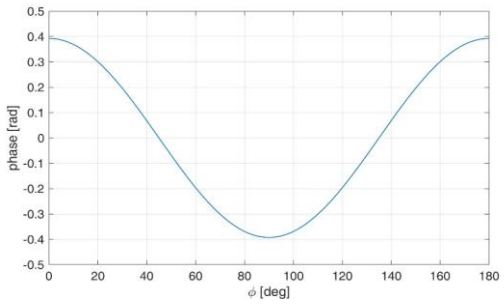

Fig. 5. Phase imbalance assumed between the two receiving channels.

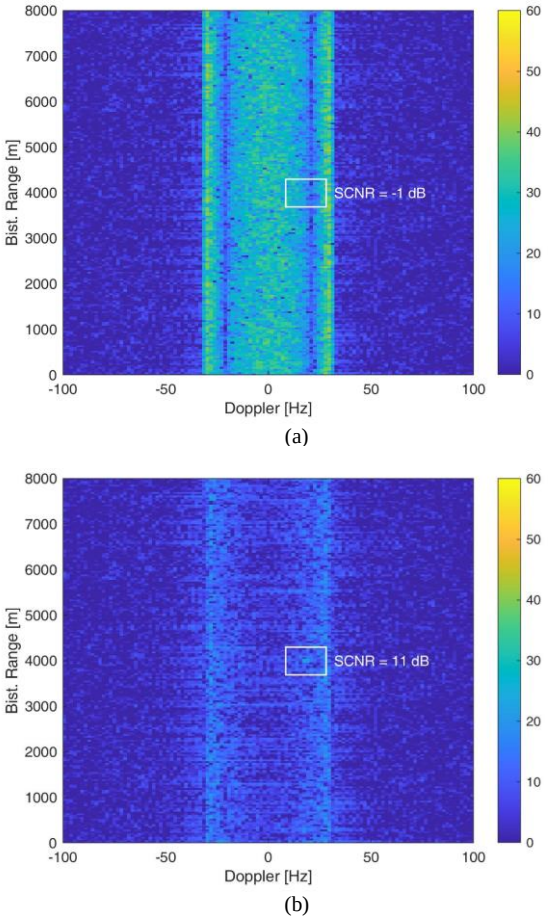

Fig. 6. Range-Doppler map after DPCA in presence of channel imbalance: (a) without channel calibration; (b) with DDC adaptive channel calibration.

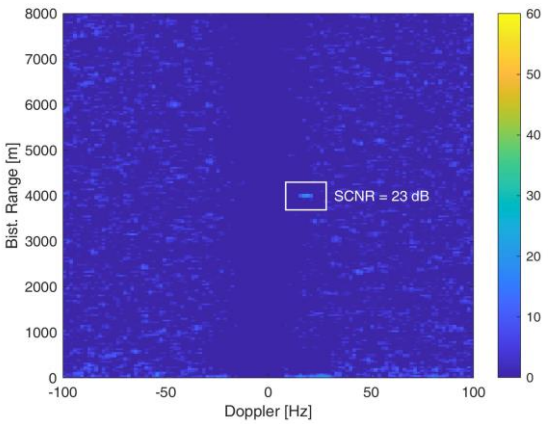

Fig. 7. Range-Doppler map after two-channels ABPD-STAP approach.

IV. Coherent and non-coherent detection schemes in presence of unknown channel imbalance

The presence of an unknown imbalance affecting the receiving channels can impact on target detection performance of a STAP approach. In fact, the mismatch of target steering vector, as well as the coefficients estimated for rejection of clutter, may result in a gain loss or even a partial suppression of target signal at the output of the adaptive filter.

It is worth noting that strategies for digital calibration of received data, like in [10], although crucial to guarantee clutter cancellation in a non-adaptive approach like DPCA, are not strictly required in the STAP case. Moreover, in case of angle-dependent imbalance, a Doppler-based calibration approach would not be useful against target steering mismatch. In fact, target signal may experience a different imbalance compared to clutter appearing at same Doppler frequencies, since belonging to a different angular direction.

If the knowledge of channel imbalance in each desired steering direction is not possible, a simple potential solution can be to renounce to a coherent integration in the spatial domain. In fact, if a small number of receiving channels is available (typically true in passive radar), this would produce a limited loss in terms of final signal to disturbance ratio.

A conventional space-time generalized likelihood ratio test (GLRT) detector, under the hypothesis of Gaussian disturbance, can be derived following the approach in [15]:

$$\frac{\left|\boldsymbol{s}^H\widehat{\boldsymbol{Q}}^{-1}\boldsymbol{x}\right|^2}{\boldsymbol{s}^H\widehat{\boldsymbol{Q}}^{-1}\boldsymbol{s}\,(1+\boldsymbol{x}^H\widehat{\boldsymbol{Q}}^{-1}\boldsymbol{x})} \gtrless \eta_1 \tag{6}$$

where η_1 is the detection threshold, which has to be selected according to the desired value of false alarm probability P_{fa}; $\boldsymbol{s}=\boldsymbol{s}_d\otimes\boldsymbol{s}_s$ is the space-time (or space-Doppler) target steering vector, being $\otimes$ the Kronecker product.
As known, such detector has the CFAR property and the analytical expression of the false alarm probability is:

$$P_{fa}=(1/l)^{K-NL+1} \tag{7}$$

where $l=1/(1-\eta_1)$.

We propose a partially non-coherent space-time GLRT detector, where the steering vector is specified in the Doppler domain but not specified in the spatial domain, resulting in a non-coherent integration of spatial dimension.

Such detector can be derived along the line of [16], where a polarimetric adaptive detection scheme is addressed, by considering the spatial component of the steering vector $\boldsymbol{s}_s$ as a vector of unknown parameters and replacing it with its maximum likelihood estimate during the derivation.

By defining the $(NL\times N)$ matrix $\boldsymbol{\Sigma}=\boldsymbol{s}_d\otimes\boldsymbol{I}_N$, where $\boldsymbol{I}_N$ is the N-dimensional identity matrix, the resulting GLRT detector is given by:

$$\frac{\boldsymbol{x}^H\widehat{\boldsymbol{Q}}^{-1}\boldsymbol{\Sigma}\left(\boldsymbol{\Sigma}^H\widehat{\boldsymbol{Q}}^{-1}\boldsymbol{\Sigma}\right)^{-1}\boldsymbol{\Sigma}^H\widehat{\boldsymbol{Q}}^{-1}\boldsymbol{x}}{(1+\boldsymbol{x}^H\widehat{\boldsymbol{Q}}^{-1}\boldsymbol{x})} \gtrless \eta_2 \tag{8}$$

This detector still has the CFAR property and the expression of the false alarm probability follows (see [16]):

$$P_{fa}=\frac{(1-\eta_2)^{K-NL+1}}{(K-NL)!}\sum_{j=1}^{N}\frac{(K-NL+N-j)!\;\eta_2^{N-j}}{(N-j)!} \tag{9}$$

In order to compare the two detection schemes, we consider a simulated clutter scenario, with same parameters of previous section and observed by $N=3$ receiving channels affected by an angle-dependent imbalance. Specifically, we assume a sinusoidal phase error between the three channels as illustrated in Fig. 8 (channel 3 is arbitrarily taken as reference). Two cases are considered with different level of fluctuation: case *a* and case *b* with maximum phase error of $\pi/4$ and $\pi/2$, respectively. A moving target is assumed, with azimuth angle of arrival $\varphi_0=90°$ and whose bistatic radial velocity is varied in the interval $[1:14]$ m/s. ABPD-STAP approach is adopted, with $L=3$ Doppler bins, for a total of $NL=9$ degrees of freedom. The number of training data is $K=54$.

Performance is analysed by directly comparing the output of the two detectors in (6) and (8), taken at target range-Doppler bin, with the corresponding thresholds, derived from (7) and (9) for different required values of P_{fa}. Results are shown, as a function of target bistatic radial velocity, in Fig. 9 (a) and (b), for the coherent and the non-coherent GLRT detector respectively. As a benchmark, the analogous case in absence of inter-channel imbalance is also considered.

For the coherent detector case (see Fig. 9(a)), a partial suppression on target is evident, due to the effect of the imbalance between channels and target steering mismatch. This effect increases as imbalance fluctuation increases from case *a* to case *b*, and results in several missing detections of the target, for the selected values of P_{fa}.

Conversely, when the non-coherent detection scheme is considered (see Fig. 9(b)), the influence of channel imbalance on target signal integration is counteracted. Clutter is still effectively cancelled, thanks to the adaptive space-time filtering of data, while the partial target suppression due to steering vector mismatch is now prevented. As a result, target detections are preserved, regardless of the imbalance level.

Notice that, when no imbalance is assumed between receiving channels, both schemes allow target detection for all considered P_{fa} values and all target velocities (except 1 m/s). However, as expected, the coherent detector shows a slightly better margin, thanks to a higher maximum integration gain.

For selected target velocities, probability of detection is estimated by means of a Monte Carlo analysis and reported in Table I, for a P_{fa} of 10^{-6}. As evident, the non-coherent scheme preserves detection capability when in presence of imbalance.

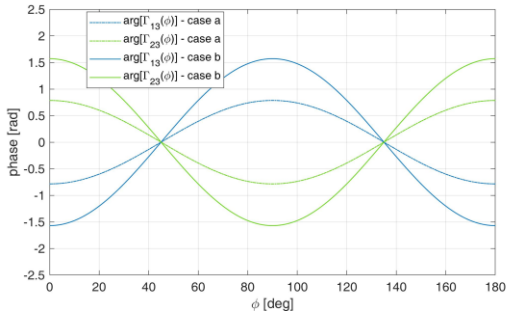

Fig. 8. Phase imbalance with different amplitudes assumed between the three receiving channels. Channel 3 is assumed as reference.

V. Conclusions

This paper addressed the problem of clutter rejection and slow-moving target detection in multichannel mobile passive radar. In particular, the impact of channel calibration issues on space-time processing algorithms was discussed.

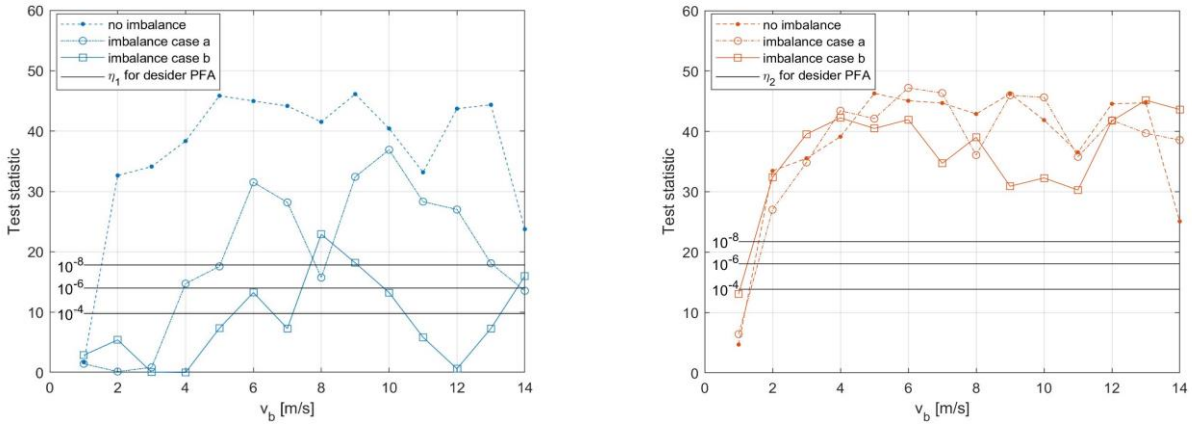

(a) (b)

Fig. 9. Test statistics of considered GLRT detectors as a function of target bistatic radial velocity: (a) coherent GLRT; (b) partially non-coherent GLRT. Corresponding thresholds for desired Pfa values are also reported.

TABLE I. ESTIMATED PROBABILITY OF DETECTION

Target velocity	Coherent GLRT			Non-coherent GLRT		
	no imbalance	imbalance case *a*	imbalance case *b*	no imbalance	imbalance case *a*	imbalance case *b*
$v_b = 7\ m/s$	0.99	0.89	0.04	0.98	0.97	0.89
$v_b = 3\ m/s$	0.64	0.01	0	0.55	0.55	0.56

The simple scheme based on DPCA approach, proposed by the authors in previous works, was firstly considered and its limitations were highlighted, when an angle-dependent imbalance affects the receiving channels. The need for an adaptive channel calibration stage, suggested to adopt a more flexible STAP solution.

At the expense of a higher computational cost, STAP offers enhanced clutter rejection capability, thanks to a higher number of adaptive degrees of freedom. Specifically, an ABPD-STAP approach was considered and its performance compared to a DPCA scheme against a simulated clutter scenario. Results confirmed the advantages of STAP, especially in the presence of an angle-dependent channel imbalance.

Finally, a space-time GLRT detection scheme was proposed, where steering vector is not specified in the spatial domain, resulting in a non-coherent integration of target echoes across the receiving channels. At the expense of a limited loss in terms of maximum integration gain and directivity (when using few receiving channels), it offers comparable clutter cancellation capability, thanks to adaptive space-time filtering, and it is more robust against losses due to target spatial steering vector mismatches, in the case of significant angle-dependent imbalance affecting the receiving channels. This solution proved to be a suitable alternative to conventional GLRT for the purpose of target detection.

REFERENCES

[1] P. Lombardo, F. Colone, "Advanced processing methods for passive bistatic radar systems", chapter in book edited by W. L. Melvin and J. A. Scheer, "Principles of Modern Radar: Advanced Radar Techniques," SciTech Publishing, Inc., 2012, pp. 739-821.

[2] R. Klemm et alii (Eds.), "Novel radar techniques and applications", Part III: Passive and multistatic radar, IET Publisher, 2017.

[3] R. Klemm, "Principles of Space-Time Adaptive Processing," IET, 2002, 3rd edn.

[4] B. Dawidowicz, P. Samczynski, M. Malanowski, J. Misiurewicz and K. S. Kulpa, "Detection of moving targets with multichannel airborne passive radar," IEEE Aerospace and Electronic Systems Magazine, pp. 42-49, 2012.

[5] B. Dawidowicz, K. Kulpa, M. Malanowski, J. Misiurewicz, P. Samczynski and M. Smolarczyk, "DPCA detection of moving targets in airborne passive radar," IEEE Transactions on Aerospace and Electronic Systems, pp. 1347-1357, April 2012.

[6] P. Wojaczek, F. Colone, D. Cristallini, P. Lombardo and H. Kuschel, "The application of the Reciprocal Filter and DPCA for GMTI in DVB-T PCL," in International Conference on Radar Systems, Belfast, 2017.

[7] P. Wojaczek, F. Colone, D. Cristallini and P. Lombardo, "Reciprocal-Filter-based STAP for passive radar on moving platforms," IEEE Transactions on Aerospace and Electronic Systems, vol. 55, no. 2, pp. 967-988, April 2019.

[8] P. Wojaczek, D. Cristallini and F. Colone, "Minimum variance power spectrum based calibration for improved clutter suppression in PCL on moving platforms," 2019 IEEE Radar Conference (RadarConf), Boston, MA, USA, 2019, pp. 1-6.

[9] G. P. Blasone, F. Colone, P. Lombardo, P. Wojaczek and D. Cristallini, "A two-stage approach for direct signal and clutter cancellation in passive radar on moving platforms," 2019 IEEE Radar Conference (RadarConf), Boston, MA, USA, 2019, pp. 1-6.

[10] G.P. Blasone, F. Colone, P. Lombardo, P. Wojaczek, D. Cristallini, "Passive radar DPCA schemes with adaptive channel calibration", submitted to IEEE Transactions on Aerospace and Electronic Systems.

[11] J. Ender, "The airborne experimental multi-channel SAR system AERII," European SAR conference (EUSAR), March 1996, pp. 49–52.

[12] C. H. Gierull, "Digital channel balancing of along-track interferometric SAR data," Defence Research and Development Canada (DRDC), Tech. Rep. TM-2003-024, 2003.

[13] P. Wojaczek, A. Summers and D. Cristallini, "Preliminary experimental results of STAP for passive radar on a moving platform," 22nd International Microwave and Radar Conference (MIKON), Poznan, 2018, pp. 589-592.

[14] J. Ward, "Space-Time Adaptive Processing for Airborne Radar", Technical Report 1015, Lincoln Laboratory, Massachusetts Institute of Technology, Lexington, MA, 1994.

[15] E. J. Kelly, "An Adaptive Detection Algorithm," in IEEE Transactions on Aerospace and Electronic Systems, vol. AES-22, no. 2, pp. 115-127, March 1986.

[16] D. Pastina, P. Lombardo and T. Bucciarelli, "Adaptive polarimetric target detection with coherent radar. Part I: Detection against Gaussian background," IEEE Transactions on Aerospace and Electronic Systems, vol. 37, no. 4, pp. 1194-1206, Oct. 2001.